

Stable-isotope changes in tufa stromatolites of the Quaternary Añamaza fluvial system (Iberian Ranges, Spain)

Los variaciones en los isótopos estables de estromatolitos tobáceos cuaternarios del sistema fluvial del Añamaza (Cordillera Ibérica, España)

M. Cinta Osácar Soriano, Concha Arenas Abad, Carlos Sancho Marcén, Gonzalo Pardo Tirapu, Leticia Martín Bello

Departamento de Ciencias de la Tierra, Universidad de Zaragoza. C/Pedro Cerbuna 12, 50009-Zaragoza (España)
cinta@unizar.es; carenas@unizar.es, csancho@unizar.es, gparado@unizar.es, leticia.martin.bello@gmail.com

ABSTRACT

The stable isotope composition ($\delta^{13}\text{C}$ and $\delta^{18}\text{O}$) of the laminae in three Quaternary, calcitic, tufa stromatolites of different ages (MIS6, MIS5 and MIS1) in the Añamaza valley are studied and compared with the modern tufa in the Añamaza river. The cyclic textural variations represent thick cyanobacterial growth in the light laminae and thin or absent cyanobacterial growth in the dark laminae. The textural cyclicity is parallel to $\delta^{18}\text{O}$ changes: Each light-dark couplet corresponds to one year in which the light lamina (lower $\delta^{18}\text{O}$ values) represents warmer water temperatures (T_w) than the dark lamina (higher $\delta^{18}\text{O}$ values). This is consistent with the fact that the large crystals composing the dark laminae correspond to precipitation in the absence of microbial films and likely represent the coldest conditions. The $\delta^{18}\text{O}_{\text{calcite}}$ -derived T_w from MIS5 stromatolite is higher than the MIS6 and MIS1 samples, which agrees with the commonly admitted climatic conditions during MIS5 in NE Iberia. Moreover, $\delta^{18}\text{O}_{\text{derived}}$ T_w from MIS6 suggests a wider yearly T_w range than the two other samples. The higher and more dispersed $\delta^{13}\text{C}$ values of the MIS1 stromatolite are consistent with the peculiarities of the vegetal cover and the decreased water availability in the Holocene.

Key-words: Stromatolite texture, stable isotopes, fluvial tufa, Pleistocene, Holocene

RESUMEN

Se estudia la composición isotópica ($\delta^{13}\text{C}$ y $\delta^{18}\text{O}$) de las láminas de tres estromatolitos calcíticos de diferente edad (MIS6, MIS5 y MIS1), en el valle del río Añamaza, y se compara con tobas actuales de este río. La variación textural cíclica representa un crecimiento cianobacteriano potente en las láminas claras y uno débil o ausente en las oscuras. Esta ciclicidad es paralela a los cambios del $\delta^{18}\text{O}$: Cada pareja clara-oscura corresponde a un año, donde la lámina clara (menor $\delta^{18}\text{O}$) representa temperatura de agua (T_w) más cálida que la lámina oscura (mayor $\delta^{18}\text{O}$). Los cristales grandes que forman las láminas oscuras precipitarían en ausencia de biofilms y posiblemente representan condiciones más frías. La T_w derivada de $\delta^{18}\text{O}_{\text{calcite}}$ en la muestra MIS5 es mayor que la T_w en las muestras MIS6 y MIS1, en consonancia con las condiciones climáticas durante el MIS5 en Iberia. Además, la T_w derivada de $\delta^{18}\text{O}_{\text{calcite}}$ en la muestra MIS6 sugiere un rango de T_w anual más amplio que en las otras dos muestras. La mayor dispersión y mayores valores de $\delta^{13}\text{C}$ en el estromatolito MIS1 son compatibles con las peculiaridades de la cobertera vegetal y la menor disponibilidad hídrica en el Holoceno.

Palabras clave: textura de estromatolitos, isótopos estables, tobas fluviales, Pleistoceno, Holoceno

Geogaceta, 61 (2017), 167-170
ISSN (versión impresa): 0213-683X
ISSN (Internet): 2173-6545

Recepción: 8 de julio de 2016
Revisión: 3 de noviembre de 2016
Aceptación: 25 de noviembre 2016

Introducción

Tufa stromatolites are considered suitable records to study high frequency environmental changes based on the stable isotope composition ($\delta^{13}\text{C}$ and $\delta^{18}\text{O}$) of the successive laminae (Andrews, 2006 and references therein). These analyses are especially useful in the study of the Quaternary climatic changes in the Mediterranean domain. However, the interpretation of the past climatic conditions based on the isotopic record is hampered by the lack of in-

formation on the isotopic composition of water and the diversity of factors that condition the isotope signature (Matsuoka *et al.*, 2001).

Monitoring of the modern tufa formation process provides useful information that helps interpret variations of the isotopic composition on different temporal scales in the geological record (Osácar *et al.*, 2013).

The purpose of this work is to interpret, in terms of environmental (mainly climatic) parameters, the isotopic variations 1) between light and dark laminae and 2)

through time of Quaternary tufa stromatolites of different ages in the Añamaza tufa system, with the help of the results of the modern tufa monitoring in the present system.

Geological context: Stratigraphy and Sedimentology

The Añamaza valley, in the Northwestern Iberian Range (NE Spain, Fig. 1A), exhibits Mid-Late Pleistocene and Holocene tufas and associated detrital facies forming

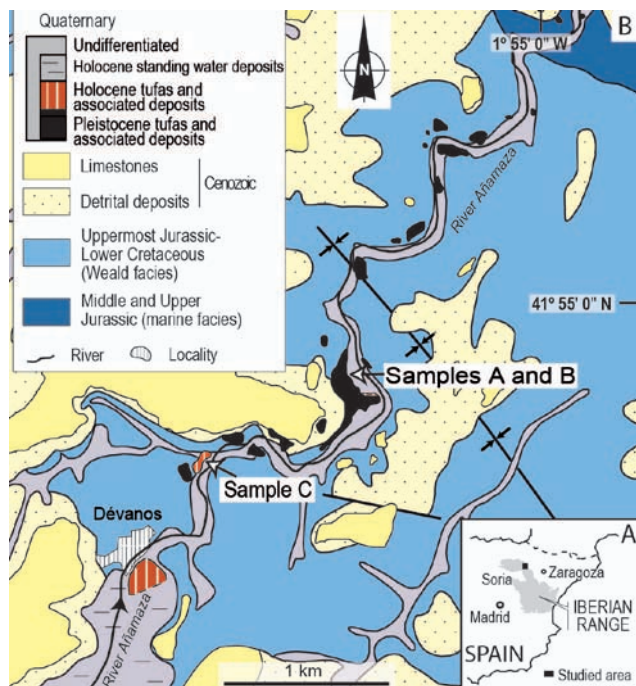


Fig. 1.-Location of the Añamaza valley and geological mapping, with Quaternary outcrops and position of the studied stromatolite samples. Modified from Arenas *et al.* (2014) and Sancho *et al.* (2015).

*Fig. 1.- Localización y cartografía geológica del valle del río Añamaza, con los afloramientos cuaternarios y la posición de los estromatolitos estudiados. Modificado de Arenas *et al.* (2014) y Sancho *et al.* (2015).*

stepped buildups, a few meters up to 70 m thick, along the valley. These Quaternary deposits lie over Mesozoic and Cenozoic rocks through an angular unconformity (Fig. 1B) (Arenas *et al.*, 2014). Several stages of tufa development in the Pleistocene (marine isotope stages, MIS9, 6 and 5) and Holocene (MIS1) have been distinguished by means of absolute datings (Arenas *et al.*, 2010; Sancho *et al.*, 2015).

The deposits consist of dominant carbonates (tufa and related facies) lying over less abundant detrital deposits formed by conglomerates and, occasionally, mudstones. The carbonate facies include: stromatolites, phytoherm tufas (bryophyte, charophyte, up growing and down-growing stem boundstones), phytoclastic tufas, oncoidal, bioclastic and intraclastic limestones, bioclastic sands and silts, massive marls and speleothems (Arenas *et al.*, 2014).

Within the general stepped carbonate fluvial context, two conceptual sedimentary models are clearly defined in the Añamaza valley (Arenas *et al.*, 2014). The moderate-slope model includes extensive standing-water areas dammed by barrage-cascades; bioclastic silts, sands and limestones, along with stem phytoherms, phytoclastic and marly, at places peaty, sediments formed in the standing water areas; abundant stem phytoherms account for extensive palustrine areas. The high-slope model consists of smaller dammed areas between close-up cascades and barrage-cascades, which were

composed primarily of moss phytoherms, stromatolites and phytoclastic tufas. For each model, the depositional bodies consist, respectively, of large and small wedges that open downstream. The sedimentological and hydrological differences between the Pleistocene and Holocene fluvial systems in the Añamaza valley can be referred, respectively, to the high-slope and moderate-slope models, but the models can coexist in a single sedimentary system (Arenas *et al.*, 2014).

The Pleistocene stromatolites studied here (164.4 ± 1.8 ka and 111.7 ± 1.7 ka, MIS6 and MIS5 respectively; Sancho *et al.*, 2015) form part of a stepped cascade developed at the downstream part of a small wedge that was deposited in a high-slope area of the valley (low aggradation/progradation ratio, Arenas *et al.*, 2014). The Holocene stromatolites studied here (7.7 ± 3.8 ka, MIS1; Sancho *et al.*, 2015) formed at the downstream part of a large wedge, in a moderate slope area of the valley that included small barrages and cascades and wide palustrine zones (Arenas *et al.*, 2014).

Materials and methods

Three samples of stromatolites were selected for stable-isotope analyses. Two samples from the Pleistocene (A, MIS6 and B, MIS5) and one sample from the Holocene (C, MIS1), spanning approximately 12 cm thick in total. Successive light and dark la-

minae were sampled with a microdrill (Fig. 2). In a few light laminae two samples were obtained vertically. A total of 42 powder samples from light laminae (13 in A, 15 in B and 14 in C) and 37 from dark laminae (13 in A, 15 in B and 9 in C) were obtained. According to the X-Ray Diffraction analyses, carried out at the University of Zaragoza, samples consist almost entirely of calcite. Texture was studied in thin sections through optical microscope and in scanning electron microscope (SEM) in the University of Zaragoza. Thin sections were prepared by the Servicio de Preparación de Rocas y Materiales Duros of the University of Zaragoza. The $\delta^{13}\text{C}$ and $\delta^{18}\text{O}$ analyses were performed in a Thermo Finnigan MAT-252 mass spectrometer in the Serveis científic-tècnics of the University of Barcelona, following standard procedures.

Results

Structure and texture of stromatolites

The Pleistocene samples were taken from multi-convex meter-thick bodies in which stromatolite (5-20 cm thick), phytoclastic tufa and bryophyte boundstone layers alternate, and the Holocene sample from a slightly undulate, 4 cm-thick body that lies over a phytoclast tufa and stem boundstone layer.

The three studied samples consist of flat to slightly undulate, locally domed, laminae (Fig. 2). Lamination is defined by an alternation of light laminae (1 to 3.5 mm thick) and dark laminae (0.2 to 1 mm thick). The light laminae correspond to micrite and spar calcite with abundant cyanobacterial fila-

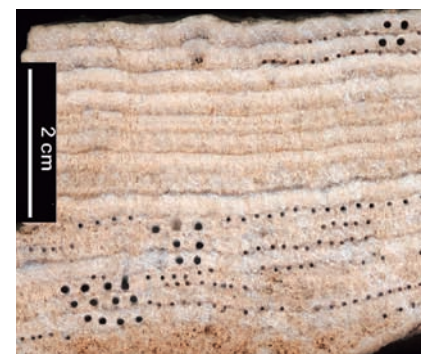


Fig. 2.-Detail of sample B (MIS5) showing alternating light and dark laminae. Microboreholes correspond to sampling.

Fig. 2.-Detalle de la muestra B (MIS5) mostrando la alternancia de láminas claras y oscuras. Las microperforaciones corresponden al muestreo.

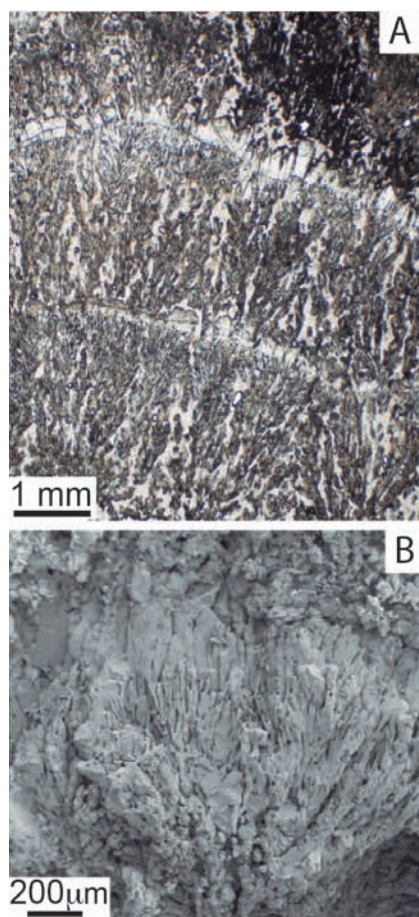


Fig. 3.-Optical microscope (A: sample C, MIS1) and SEM (B: sample A, MIS6) images of the studied stromatolite laminae.

Fig. 3.-Imágenes de microscopio óptico (A: nuestra C, MIS1) y electrónico (B: muestra A, MIS6) de las láminas estromatolíticas estudiadas.

mentous bodies (calcite tubes in SEM) that are arranged as palisades, commonly as adjacent bush or fan-shaped bodies. The dark laminae consist of large calcite crystals (up to 0.5 mm long) that are set perpendicular to lamination and that develop on top of the light laminae. The boundaries between these types of laminae can be both sharp and gradual (Fig. 3A and B).

Stable isotopes

$\delta^{13}\text{C}$ values range from -3.96 to -6.45‰ V-PDB. Means and standard deviations of $\delta^{13}\text{C}$ for each sample are shown in table I and figure 4. Differences between the mean values of light and dark laminae are small in the Pleistocene samples (0.11 in A and 0.01‰ in B), and higher in the Holocene (0.36‰ in C), with mean values of the dark laminae slightly more negative than those of the light laminae.

$\delta^{18}\text{O}$ values range from -6.82 to -9.27‰ V-PDB. Means and standard deviations of $\delta^{18}\text{O}$ for each sample are shown in table I and figure 4. Differences between the light and dark laminae are 0.94, 0.51 and 0.21‰ in A, B and C, respectively. In all cases, the dark laminae have significantly less negative values than the light laminae.

The correlation between $\delta^{13}\text{C}$ and $\delta^{18}\text{O}$ is absent or very poor ($r = 0.23, 0.06$ and 0.30 , for A, B and C, respectively).

Discussion

The textural variations are cyclic and represent thick cyanobacterial growth in the light laminae and thin or absent cyanobacterial growth in the dark laminae (Fig. 3). The large crystals of the dark laminae are primary precipitates and likely correspond to precipitation in the absence of microbial films (cf., Arp *et al.*, 2010). The textural cyclicity can be, thus, interpreted as a function of seasonal variations in microbial growth associated with climate parameters. The oscillation of $\delta^{18}\text{O}$, with lower values in the light laminae and higher values in the dark laminae, represents seasonal changes in water temperature (Tw). Following the temperature dependence of the oxygen fractionation, the thinner, dark laminae formed with lower Tw, and the thicker, light laminae with higher Tw. All together, these facts suggest that every light-dark couplet likely represents a year, whose Tw oscillation is reflected in the $\delta^{18}\text{O}$ values of each light and dark couplet. Nevertheless, it cannot be inferred that the two types of laminae represent similar time spans, but intervals with dominant warm and cool conditions.

Assuming each couplet represents a year, the Holocene sample (C, MIS1) represents 9 years and the Pleistocene samples represent 15 years (B, MIS5) and 13 years (A, MIS6). Sedimentation rates for the three samples, calculated from the above data, are similar (2.5 to 2.6 mm/y).

The $\delta^{13}\text{C}$ and $\delta^{18}\text{O}$ composition of the studied samples are in the range of other recent and ancient carbonate fluvial systems (Andrews, 2006; Brasier *et al.*, 2010; Domínguez-Villar *et al.*, 2012). The calcite $\delta^{18}\text{O}$ of the studied samples is slightly higher than the $\delta^{18}\text{O}$ of recent tufa in the Añamaza river (mean $\delta^{18}\text{O} = -8.7\text{‰}$ V-PDB, Auqué *et al.*, 2014). In turn, the $\delta^{13}\text{C}$ is lower than the

recent tufa (mean $\delta^{13}\text{C} = -7.3\text{‰}$ V-PDB, Auqué *et al.*, 2014). However, whereas the value of the offset between the Pleistocene samples and the recent tufa is similar to the $\delta^{13}\text{C}$ decrease in the atmosphere due to the Suess effect (-1.5‰ PDB, Keeling, 1979), the Holocene tufa $\delta^{13}\text{C}$ is significantly higher than the recent and the Pleistocene $\delta^{13}\text{C}$. This difference is consistent with the peculiarities of the Holocene vegetal cover, related to the insolation and the vegetation distribution derived from the Last Glacial Maximum (García-Prieto, 2015).

A decrease in the water availability in the Holocene relative to the Mid-Late Pleistocene, supported by sedimentological data and bulk stable-isotope data of the Quaternary record in this valley, led to similar conclusions (Arenas *et al.*, 2014). A decrease in precipitation from the early Holocene onwards has also been observed in Iberia (Domínguez-Villar *et al.*, 2012). The low $\delta^{13}\text{C}$ has also been related to increases in discharge (Lojen *et al.*, 2009) and, locally, with biotic vs. abiotic processes (Souza-Egypsy *et al.*, 2006).

The calcite $\delta^{18}\text{O}$ variations can be interpreted in terms of Tw change. Mean global $\delta^{18}\text{O}$ values of MIS6 and MIS1 samples are similar, whereas MIS5 values correspond to higher temperatures (Table I). Assuming a change of 0.24‰ in calcite $\delta^{18}\text{O}$ per 1°C in Tw, the mean Tw difference between these two groups is about 2.5°C. This higher temperature inferred from tufa $\delta^{18}\text{O}$ is coherent with the general more favorable conditions for tufa formation during MIS5 in NE Iberia (Sancho *et al.*, 2015).

	$\delta^{13}\text{C}$ ‰ (VPDB)	$\delta^{18}\text{O}$ ‰ (VPDB)
Holocene (MIS1) Sample C		
Light laminae	-4.92 (0.53)	-8.08 (0.38)
Darklaminae	-5.28 (0.68)	-7.87 (0.62)
Wholesample	-5.11 (0.60)	-7.98 (0.50)
Pleistocene (MIS5) Sample B		
Light laminae	-6.03 (0.35)	-8.84 (0.25)
Darklaminae	-6.02 (0.24)	-8.33 (0.33)
Wholesample	-6.03 (0.29)	-8.59 (0.39)
Pleistocene (MIS6) Sample A		
Light laminae	-6.14 (0.16)	-8.46 (0.32)
Darklaminae	-6.03 (0.17)	-7.52 (0.52)
Wholesample	-6.08 (0.17)	-7.99 (0.63)

Table I.- Means and standard deviations of $\delta^{13}\text{C}$ and $\delta^{18}\text{O}$ values of the studied samples.

Tabla I.- Valores medios y desviaciones típicas de $\delta^{13}\text{C}$ y $\delta^{18}\text{O}$ de las muestras estudiadas.

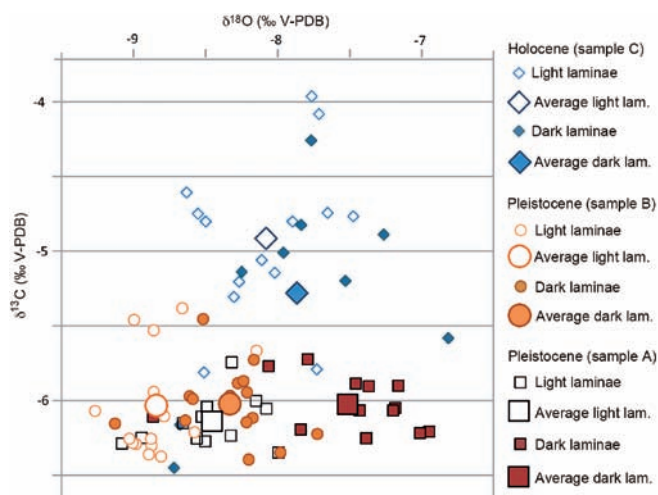


Fig. 4.- $\delta^{13}\text{C}$ vs $\delta^{18}\text{O}$ of the studied samples.

Fig. 4.- $\delta^{13}\text{C}$ vs $\delta^{18}\text{O}$ de las muestras estudiadas.

The respective MIS6 and MIS5 $\delta^{18}\text{O}$ values of light and dark laminae reflect also different temperature range: the difference between dark and light laminae would correspond to ca. 4°C in MIS6 sample, and 2.1°C in the MIS5 sample. The MIS1 sample temperature range is even smaller, 0.9°C. However, the actual Tw range through the year might be larger, taking into account the influence of the seasonal changes in water $\delta^{18}\text{O}$ signature. Sedimentation monitoring of the Añamaza River (from 2007 to 2010) showed a significant difference between the present water $\delta^{18}\text{O}$ of the warm and cool seasons (ca. 0.5‰). This seasonal water $\delta^{18}\text{O}$ difference may cause a narrowing in the calcite $\delta^{18}\text{O}$ range of these deposits that formed at very different Tw. In the Añamaza modern tufa, with a mean difference of 0.1‰ between calcite $\delta^{18}\text{O}$ of the warm and cool seasons, the calculated Tw difference was ca. 6°C (Auqué *et al.*, 2014).

The dispersion of $\delta^{13}\text{C}$ values in the MIS1 sample is larger than in the MIS6 and MIS5 samples (Fig. 4), which is difficult to interpret, due to the diversity of processes involved in the calcite $\delta^{13}\text{C}$ signature.

Conclusions

Textural features of lamination and stable-isotope composition of Pleistocene (MIS5 and MIS6) and Holocene (MIS1) tufa stromatolites of the Añamaza valley indicate the development of a biannual lamination pattern, with light laminae mostly reflecting the warm interval and dark laminae the cold interval.

Lamination is controlled by seasonal variations in the cyanobacterial growth that are parallel to oscillations of $\delta^{18}\text{O}$ values, reflecting biannual changes in water temperature. According to calcite $\delta^{18}\text{O}$, the MIS5 stromatolite corresponds to higher temperature than the MIS6 and MIS1 samples; moreover, MIS6 sample suggests a higher yearly temperature range than the two other samples. As it has been observed in the recent tufas, the seasonal variability of the water $\delta^{18}\text{O}$ must be taken into account to interpret the actual temperature range, which can be larger than the directly inferred from the calcite $\delta^{18}\text{O}$ range.

$\delta^{13}\text{C}$ values for the Holocene tufa are higher and more disperse than those measured in the Pleistocene samples. This difference may be associated with peculiarities in the vegetal cover and with the decreased water availability in the Holocene relative to the Late Pleistocene.

Acknowledgements

This study was funded by projects CGL2006-05063/BTE, CGL2009-09216/BTE and CGL-2013-42867-P of the Spanish Government and European Regional Development Fund. It is a contribution of the research groups *Continental sedimentary Basin Analysis, PaleoQ, Geotransfer* and *GMG* of the Government of Aragón-UNIZAR and IUCA. Our gratitude to the reviewers M. Esther Sanz Montero and M^a A. García del Cura for their valuable comments

References

- Andrews, J.E. (2006). *Earth-Science Reviews* 75, 85-104.
- Arenas, C., Sancho, C., Vázquez-Urbez, Pardo, G., Hellstrom, J., Ortiz J.E., de Torres, T., Osácar, M.C. and Auqué, L. (2010). *Geogaceta* 49, 51-54.
- Arenas, C. Vázquez-Urbez, M., Pardo, G. and Sancho, C. (2014). *Sedimentology* 61, 133-171.
- Arp, G., Bissett, A., Brinkmann, N., Cousin, S., De Beer, D., Friedl, T., Mohr, K.I., Neu, T.R., Reimer, A., Shiraishi, F., Stackebrandt, E. and Zippel, B. (2010). *Geological Society, London, Special Publication* 336, 83-118.
- Auqué, L., Arenas, C., Osácar, C., Pardo, G., Sancho, C. and Vázquez-Urbez, M., (2014). *Sedimentary Geology* 303, 26-48.
- Brasier, A.T., Andrews, J.E., Marca-Bell, A.D. and Dennis, P.F. (2010). *Global and Planetary Change* 71, 160-167.
- Domínguez-Villar, D., Vázquez-Navarro, J.A. and Carrasco, R.M. (2012). *Geomorphology* 161-162, 15-25.
- García-Prieto, E. (2015). *Dinámica paleoambiental durante los últimos 135.000 años en el Alto Jiloca: el registro lacustre de El Cañizar*. Tesis Doctoral, Universidad de Zaragoza, 332 p.
- Keeling, C.D. (1979). *Environment International* 2 (4-6), 229-300.
- Lojen, S., Trkov, A., Scancar, J., Vazquez-Navarro, J.A. and Cukrov, N. (2009). *Chemical Geology* 258, 242-250.
- Matsuoka, J., Kano, A., Oba, T., Watanabe, T., Sakai, S. and Seto, K. (2001). *Earth and Planetary Science Letters* 192, 31-44.
- Osácar, C., Arenas, C., Vázquez-Urbez, M., Sancho, C., Auqué, L.F. and Pardo, G. (2013). *Journal of Sedimentary Research* 83, 309-322.
- Sancho, C., Arenas, C., Vázquez-Urbez, M., Pardo, G., Lozano, M.V., Peña, J.L., Hellstrom, J., Ortiz, J.E., Osácar, M.C., Auqué, L. and Torres, T. (2015). *Quaternary Research* 84 (3), 398-414.
- Souza-Egypsy, V., García del Cura, M.A., Ascaso, C., De los Ríos, A., Wierzbos, J. and González-Martín, J.A. (2006). *International Review of Hydrobiology* 91, 222-241.